

Physical Characterization and Platelet Interactions under Shear Flows of a Novel Thermoset Polyisobutylene-based Co-polymer

Jawaad Sheriff,[†] Thomas E. Claiborne,[†] Phat L. Tran,[‡] Roshni Kothadia,[†] Sheela George,[†] Yasushi P. Kato,[§] Leonard Pinchuk,[§] Marvin J. Slepian,^{†,‡,⊥} and Danny Bluestein^{*,†}

[†]Department of Biomedical Engineering, Stony Brook University, Stony Brook, New York 11794-8151, United States

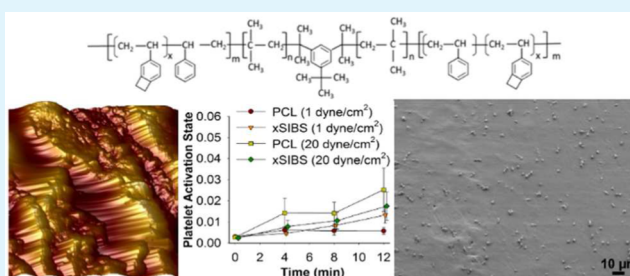
[‡]Department of Biomedical Engineering, University of Arizona, Tucson, Arizona 85721, United States

[§]Innovia LLC, Miami, Florida 33186, United States

[⊥]Sarver Heart Center, University of Arizona, Tucson, Arizona 85721, United States

ABSTRACT: Over the years, several polymers have been developed for use in prosthetic heart valves as alternatives to xenografts. However, most of these materials are beset with a variety of issues, including low material strength, biodegradation, high dynamic creep, calcification, and poor hemocompatibility. We studied the mechanical, surface, and flow-mediated thrombogenic response of poly(styrene-*coblock*-4-vinylbenzocyclobutene)-polyisobutylene-poly(styrene-*coblock*-4-vinylbenzocyclobutene) (xSIBS), a thermoset version of the thermoplastic elastomeric polyolefin poly(styrene-*block*-isobutylene-*block*-styrene) (SIBS), which has been shown to be resistant to in vivo hydrolysis, oxidation, and enzymolysis. Uniaxial tensile testing yielded an ultimate tensile strength of 35 MPa, 24.5 times greater than that of SIBS. Surface analysis yielded a mean contact angle of 82.05° and surface roughness of 144 nm, which was greater than for poly(ϵ -caprolactone) (PCL) and poly(methyl methacrylate) (PMMA). However, the change in platelet activation state, a predictor of thrombogenicity, was not significantly different from PCL and PMMA after fluid exposure to 1 dyn/cm² and 20 dyn/cm². In addition, the number of adherent platelets after 10 dyn/cm² flow exposure was on the same order of magnitude as PCL and PMMA. The mechanical strength and low thrombogenicity of xSIBS therefore suggest it as a viable polymeric substrate for fabrication of prosthetic heart valves and other cardiovascular devices.

KEYWORDS: parallel plate flow chamber, hemodynamic shearing device, thrombin, SIBS, polymers



1. INTRODUCTION

The thermoplastic elastomer polyolefin poly(styrene-*block*-isobutylene-*block*-styrene) (SIBS) has been thoroughly described and successfully utilized in commercial medical applications.¹ SIBS has been shown to be “super-biostable”, that is, without evidence of in vivo hydrolysis, oxidation, or enzymolysis.¹ However, as a thermoplastic, SIBS has limited utility due to its high dynamic creep, especially in applications subject to dynamic loading.² It was tested for use as a biomaterial in the development of novel trileaflet polymeric prosthetic heart valves (PPHV), in which SIBS was used as a coating for an underlying and reinforcing polyester mesh (SIBS-Composite), but to no avail.^{3–6} However, hemocompatibility tests confirmed the low thrombogenic potential of SIBS in that application, especially in the presence of human platelets under shear flows.^{3,7–9} To overcome the mechanical limitations of SIBS, we developed a novel thermoset formulation. Copolymerization of 4-vinylbenzocyclobutene (4-VBCB) comonomer units into the polystyrene-based hard segments of SIBS yielded poly(styrene-*coblock*-4-vinylbenzocyclobutene)-polyisobutylene-poly(styrene-*coblock*-4-vinylbenzocyclobutene) triblock copolymer, which is capable of postpolymerization,

thermal cross-linking via a Diels–Alder-like reaction involving the benzocyclobutene moieties (Figure 1). This cross-linked version of SIBS (xSIBS; U.S. Patent No. 8,765,895¹⁰) may be a viable biomaterial in applications where chronic cyclic loading of the material is expected, such as in PPHVs. As such, xSIBS promises to be a useful fabrication material for the development of an effective alternative to xenograft-based valves, which are prone to calcification and degradation.^{11,12} The modulation of the ratio of styrene-to-isobutylene and 4-VBCB-to-isobutylene produces harder (more styrene, 4-VBCB, or both) or softer (less styrene, 4-VBCB, or both) materials, with an optimum ratio for different applications. Here, we present our experience with xSIBS in PPHV development. Further, our findings emphasize the potential utility of xSIBS for other clinical applications.

We have developed a functionally and hemodynamically optimized PPHV using xSIBS.^{13,14} The advantage of the use of xSIBS in PPHVs is that it can be thermo-compression molded

Received: August 6, 2015

Accepted: September 16, 2015

Published: September 23, 2015

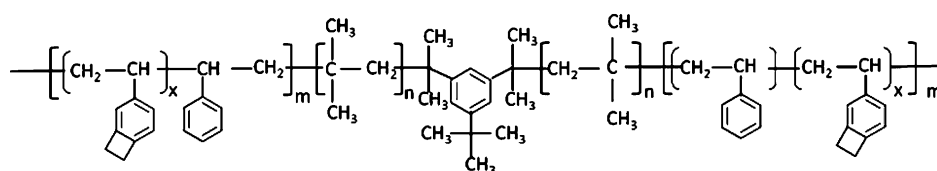


Figure 1. Schematic of poly(styrene-coblock-4-vinylbenzocyclobutene)-polyisobutylene-poly(styrene-coblock-4-vinylbenzocyclobutene) (xSIBS).

to form the valve structure and is cross-linked in the mold. This has allowed for design modifications that were not previously achievable by casting or dip-coating,⁶ leading to an optimized stress distribution within the leaflet under physiologic cardiac loading.¹³ This design novelty has predicted higher durability for an xSIBS PPHV compared to SIBS-Composite and near equivalence to xenograft material.¹³ To date, no one has been successful in developing a clinically viable PPHV, mainly due to a persistent use of polyurethanes and designs^{15,16} that have proven to be unsuitable for use in PHVs.¹⁷ While there are some promising nanocomposite polyurethanes being tested,¹⁸ long-term data are currently not available. Alternatively, xSIBS, with its SIBS-like enhanced biostability, coupled with significantly strengthened mechanical properties, may be a successful PPHV biomaterial. Furthermore, with the advent of transcatheter aortic valve replacement (TAVR),¹⁹ a transcatheter PPHV made from xSIBS may better withstand the procedural stresses that damage xenograft leaflets.^{20–24} Taking advantage of the moldability of xSIBS enables optimized transcatheter PPHV designs that may translate to better clinical outcomes than those achievable with current xenograft-based devices.¹⁷ The success of a PPHV will be a significant synthetic biomaterial milestone and another step forward from the use of present xenografts with their inherent limitations.

Here, we present results and analysis of the physical characterization and platelet interactions of molded xSIBS sheets subjected to shear flows. We performed several measurements to characterize the physical properties of xSIBS and examined the biomaterial effects on human platelets under two different *in vitro* experimental shear flow conditions: parallel plate flow and in a cone–plate–Couette viscometer. Shear stress-induced platelet activation and adhesion are major contributors to thrombosis in cardiovascular biomaterials and are functions of shear stress magnitude and exposure time.^{25–29} The mechanical, surface, and flow-mediated platelet response examinations conducted in this study significantly add to our understanding of the hemocompatibility of xSIBS as a viable PPHV polymeric material substrate.

2. MATERIALS AND METHODS

2.1. Preparation of Material Specimens. Sheets of xSIBS approximately 100 μm thick were compression-molded from raw 25% styrene content xSIBS with 2% by weight benzocyclobutene (BCB) as the cross-linker (Innovia LLC, Miami, FL) and thermally cross-linked via a Diels–Alder-like reaction¹⁰ at 240 $^{\circ}\text{C}$ for 30 min, as previously described.^{13,14} For structural, platelet activation, and platelet adhesion comparison, we also prepared poly(ϵ -caprolactone) (PCL) and poly(methyl methacrylate) (PMMA) samples. PCL has been examined as a potential scaffold material for tissue-engineered aortic valves³⁰ with low platelet adhesion after 2 h on an orbital shaker.³¹ Compared to other polymers used in cardiovascular applications, PMMA has yielded higher P-selectin,³² thrombin generation,³³ and platelet adhesion.^{32–34} PCL (MW = 80 000; PURAC Biomaterials, Lincolnshire, IL) was prepared 20% (w/v) in dichloromethane and was spin-coated onto 2.25 in. diameter glass discs (McMaster-Carr, Robbinsville, NJ) and regular microscope slides at 400 rpm for 8 s, followed by

1000 rpm for 45 s. Coated glass discs and slides were then hot baked for 1 min at 95 $^{\circ}\text{C}$ to evaporate the solvent. Glass discs and slides were spin-coated with PMMA in solution phase (MW = 950 000; MicroChem Corp., Newton, MA) at 400 rpm for 45 s, followed by 1000 rpm for 15 s, and hot baked at 180 $^{\circ}\text{C}$ for 1 min to evaporate the thinner solvent. All materials were rinsed several times with double-distilled H_2O and once with phosphate-buffered saline (PBS) prior to *in vitro* experiments.

2.2. Material Characterization. **2.2.1. ATR-FTIR and Tensile Testing Measurements.** As-cast and platelet-exposed xSIBS were characterized using Attenuated Total Reflectance Fourier Transform Infra-Red (ATR-FTIR) spectroscopy (Nicolet 370, Thermo Fisher Scientific Inc., Waltham, MA) for polymer degradation or deterioration. Samples were pressed onto a Zinc Selenide crystal at 12 psi. Each spectrum was the average of 32 scans collected over the spectral range of 500 to 4000 wavenumbers (cm^{-1}). Raw data was exported for further comparison analysis. Uniaxial tensile testing was performed on xSIBS samples according to ASTM D882-12/D638-10 standard at a 5 mm/min pull rate, as previously described.¹³

2.2.2. Water Contact Angle Measurements. The hydrophobicity or wettability of as-cast and platelet-exposed xSIBS was analyzed in comparison to PCL and PMMA by using an optical contact angle meter (CAM 100, KSV Instruments LTD, Helsinki, Finland). A drop of water, approximately 25 μL , was dispensed on the flat platform using a 3 mL syringe with 18G Luer Stub Adapter (Becton Dickinson, Franklin Lakes, NJ). Once the droplet was stabilized, six images were taken for curve fitting using the Young–Laplace equation. Left and right contact angles were analyzed. The analysis was repeated three times, and an average contact angle with standard deviation (S.D.) was reported.

2.2.3. AFM Measurements. Surface topography of as-cast and platelet-exposed xSIBS was also analyzed and compared to PCL and PMMA. The 3D topographical images were taken with an atomic force microscope (AFM, Dimension 3100, Bruker Biosciences Corp., Billerica, MA) in tapping mode with silicon probes (ACTA, Applied Nanostructures, Inc. Mountain View, CA). The images were then analyzed using the Bruker Nanoscope Analysis software (v1.40). The images were corrected using the third order flattening tool to remove tilts and bows from the image. Roughness (Ra) values were obtained using the roughness tool included in the software.

2.3. Platelet Preparation. Whole blood, 30 mL, was drawn from consenting healthy adult human subjects of both genders and anticoagulated with 10% acid citrate dextrose, solution A (ACD-A). The protocol for the study, 2012–4427-FAR-3, was approved April 12, 2013, by the Stony Brook University IRB Committee on Research Involving Human Subjects. Platelet-rich plasma (PRP) was obtained by centrifugation at 650g for 4.5 min. Platelet-poor plasma was prepared from a small volume of PRP by centrifuging at 10 000 rpm for 30 s and discarding the platelet pellet. For platelet adhesion experiments, PRP was diluted to a platelet count of 450 000/ μL in platelet-poor plasma. Gel-filtered platelets (GFP) were collected after passing PRP through a column of Sepharose 2B beads (Sigma-Aldrich, St. Louis, MO).³⁵ For platelet activation experiments, GFP were diluted to a count of 20 000/ μL in HEPES-buffered modified Tyrode's solution with Mg^{2+} and K^+ added ("platelet buffer"). The platelet solution was mixed with 3 mM Ca^{2+} 10 min prior to experiments.^{26,35}

2.4. Fluid Shear-Induced Platelet Activation. Gel-filtered platelets were exposed to the materials under fluid shear stress in the Hemodynamic Shearing Device (HSD, Figure 2), a computer-programmable cone–plate–Couette viscometer that can uniformly apply both constant and dynamic fluid shear stresses and allows for

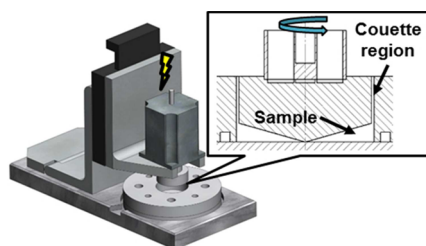


Figure 2. Shear exposure in the Hemodynamic Shearing Device (HSD). GFP suspended over the biomaterials were exposed to 1 dyn/cm² and 20 dyn/cm² for 12 min in the HSD, a computer-programmable cone–plate–Couette viscometer that exposes platelets to uniform shear stress and allows for real-time sampling.

real-time platelet sampling.^{25,36} Use of GFP in the absence of plasma proteins allows observation of the direct relationship between fluid shear and thrombin generation without platelet aggregation and adhesion. The platelet-contacting parts of the HSD are constructed of ultrahigh molecular weight polyethylene (UHMWPE) and were coated with Sigmacote (Sigma-Aldrich, St. Louis, MO) 5 min prior to experiments. xSIBS sheets were cut and adhered onto a 2.25 in. diameter glass disc (McMaster-Carr, Robbinsville, NJ). PCL and PMMA were coated onto the glass discs as described earlier. The discs were placed on the plate of the HSD and secured with a static ring. A small volume, 2 mL, of the platelet mixture was added to the material. The movable cone was adjusted to a height of approximately 20 μm above the material using a micrometer. The platelet mixture was exposed to 1 dyn/cm² or 20 dyn/cm² for 12 min, with 25 μL samples withdrawn every 4 min for a chemically modified prothrombinase-based platelet activation state (PAS) assay.^{35,37} The PAS assay measures the generation of modified thrombin that does not participate in the positive platelet activation feedback loop and therefore acts as global marker of platelet activation. The PAS assay has been shown to correlate well with P-selection expression as measured by flow cytometry.³ PAS values were normalized by those obtained after sonication at 10 W for 10 s (Branson Sonifier 150, Branson, MO). Thus, PAS values are reported as a fraction of the maximum thrombin-generating potential of the platelet mixture. In addition, experiments were not performed if the baseline PAS, prior to shear and material exposure, exceeded 1% of the sonicated PAS value. The change in PAS, ΔPAS , was calculated over the 12 min experimental duration and compared for the three materials using one-way ANOVA with Tukey's post hoc comparison. Significance was achieved for $p < 0.05$. In addition, platelet count was measured before and after shear exposure to ensure no reduction due to lysis or adhesion.

2.5. Fluid Shear-Induced Platelet Adhesion. We designed an acrylic parallel plate flow chamber with a 0.25 \times 25 \times 75 mm flow region (Figure 3A). The inflow and outflow conduits start at 1.5 mm and flare out to 9.9 mm. Polypropylene elbow connectors and silicone

tubing attach the chamber to a syringe pump (NE-1010, New Era Pump Systems Inc., Farmingdale, NY) and a reservoir (Figure 3B). The material (xSIBS sheet or PCL/PMMA coated on a standard microscope slide) was sandwiched between the upper plate, containing the flow region and microscope viewing window, and a solid lower acrylic plate. The two plates were secured using nylon screws, and the setup was mounted on a Nikon Eclipse upright phase contrast microscope with a 40 \times plan fluor objective lens (NA = 0.60, Nikon Inc., Melville, NY). The material and chamber were gently prewashed with HEPES-buffered saline (HBS), and air bubbles were removed from the system via a syringe connected to a three-way stopcock between the pump and chamber. PRP was drawn into a 10 mL disposable polypropylene syringe (Franklin Lakes, NJ). PRP was perfused into the chamber at a flow rate of 1.125 mL/min, corresponding to a wall shear stress of 10 dyn/cm², for 5 min. Flowing platelets were visualized at 100 fps using a sCMOS camera (Zyla 5.5, Andor Technology, Belfast, U.K.) connected to the NIS-Elements imaging software (Nikon Inc., Melville, NY). At the conclusion of the experiment, the chamber was gently flushed with HBS at 0.56 mL/min until no floating cells were visible. This was followed by 4% glutaraldehyde in H₂O for 1 min. The pump was then stopped, and the glutaraldehyde was allowed to settle for a total duration of 30 min. Following the fixing process, the setup was disassembled, the material was removed, and excess glutaraldehyde was gently drained. The material was gently washed with double-distilled H₂O and passed through an ethanol dehydration series (EtOH percentages of 0, 25, 50, 75, and 100%), with 5 min at each stage. At the conclusion of the dehydration series, material samples were prepared for scanning electron microscopy (SEM). The material sheets and slides were mounted on an aluminum stub and sputter-coated with 6 nm islanded gold particles in an argon chamber. Then, the samples were imaged at an extra high tension (EHT) voltage of 2 kV and 2,000 \times zoom. Adhered platelets were then counted using the Cell Counter plug-in in ImageJ (U.S. National Institutes of Health, Bethesda, MD). The number of adhered platelets was compared between the three materials using one-way ANOVA with Tukey's post hoc test, where $p < 0.05$ was considered significant.

3. RESULTS

3.1. Characterization of xSIBS. For both platelet-exposed and as-cast samples, ATR-FTIR identifies C–H and C–C bonds that are hallmarks of the styrene and isobutylene structures of xSIBS (Figure 4A). A sharp peak is observed at 1160 cm⁻¹ for the platelet-exposed xSIBS but not for the as-cast sample. This identifies C–O bonds, which may originate from cellular material. Uniaxial tensile testing achieved an ultimate tensile strength (UTS) of 35 MPa ($n = 6$), with the xSIBS sample displaying nonlinear hyperelastic stress–strain behavior up to the breaking point (Figure 4B).

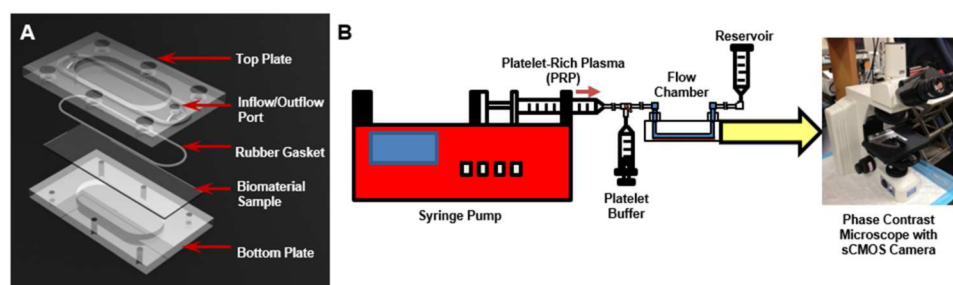


Figure 3. Parallel plate flow chamber system for platelet adhesion studies. (A) PRP was exposed to 10 dyn/cm² for 5 min in a custom parallel plate flow chamber, with channel dimensions of 75 \times 25 \times 0.1 mm. (B) The flow was controlled by a syringe pump with a 10 mL syringe that perfused PRP at 1.125 mL/min through the flow chamber into a reservoir. The flow was monitored via a 420 fps sCMOS camera mounted on a Nikon Eclipse ME600 microscope with 40 \times lens.

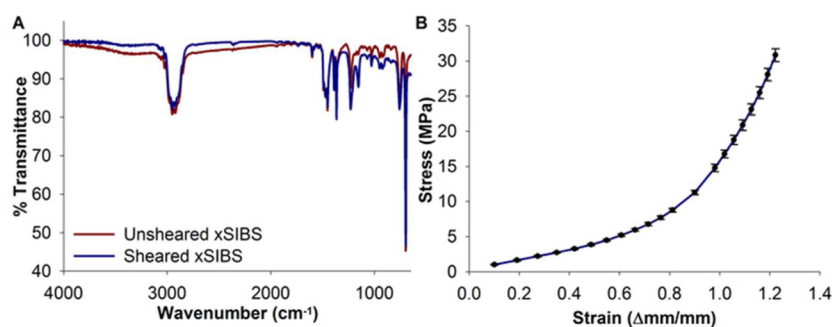


Figure 4. Material and mechanical characterization of xSIBS. (A) ATR-FTIR spectroscopy was performed on samples of xSIBS with 25% styrene content that were either unused or had been exposed to GFP and fluid shear stress of 20 dyn/cm² for 12 min in the HSD. A divergence region at 1160 cm⁻¹ indicates C–O bonds on the used xSIBS sample. (B) Tensile testing results for 6 xSIBS specimens indicate nonlinear hyperelastic behavior, with ultimate tensile strength at approximately 35 MPa.

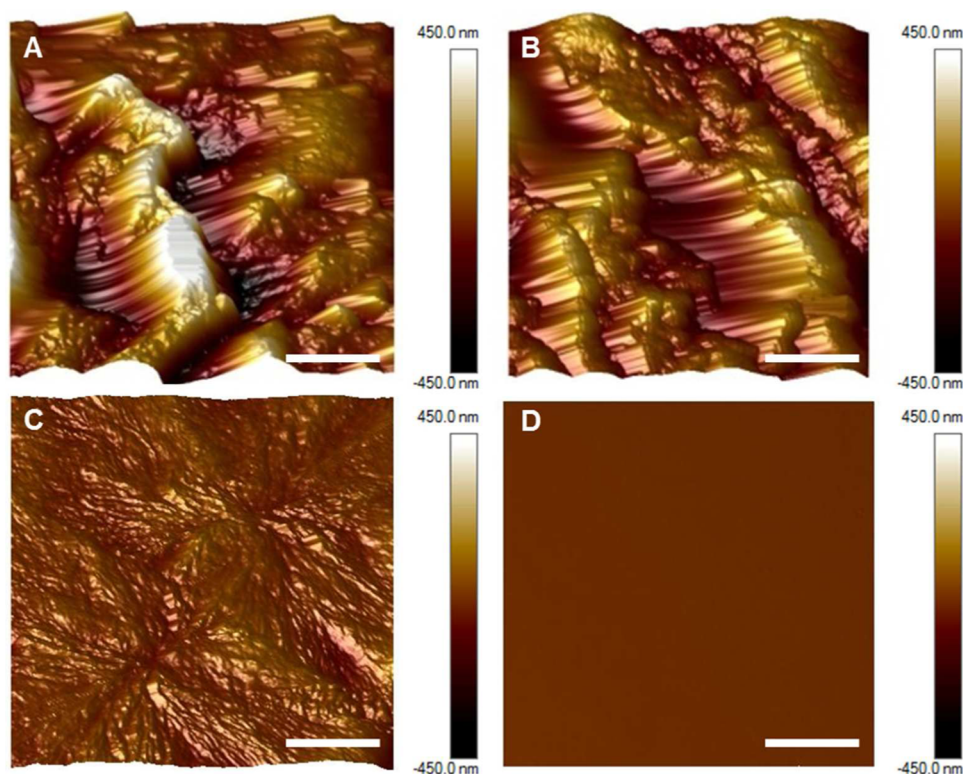


Figure 5. Surface analysis of xSIBS, PCL, and PMMA. AFM images taken of 20 × 20 μm sections of (A) as-cast 25%-styrene xSIBS, (B) platelet-exposed 25%-styrene xSIBS, (C) PCL, and (D) PMMA (5 μm lateral scale bar). Ordered styrene cylinder peaks with globular isobutylene valleys were observed on xSIBS. PMMA exhibited the lowest roughness.

Contact angles of $82.05 \pm 0.015^\circ$ and $88.27 \pm 0.04^\circ$ were measured for the as-cast and platelet-exposed xSIBS samples, respectively, indicating hydrophobicity. Greater wettability was observed for PCL and PMMA, with contact angles of $75.68 \pm 0.3^\circ$ and $70.13 \pm 0.04^\circ$, respectively ($n = 6$). Significance, as calculated using Kruskal–Wallis ANOVA, was observed for (1) PMMA versus as-cast xSIBS ($p < 0.05$), (2) PMMA versus platelet- and flow-exposed xSIBS ($p < 0.001$), and PCL versus platelet- and flow-exposed xSIBS ($p < 0.05$). AFM images of 20 × 20 μm sampled regions show that as-cast xSIBS (Figure 5A) and platelet-exposed xSIBS (Figure 5B) are characterized by large peaks and valleys that are not as evident on PCL (Figure 5C), and not present on PMMA (Figure 5D). Segmentation is observed on both xSIBS and PCL, whereas PMMA shows a single phase amorphous form. Further analysis of these images

yield Ra values of 144 nm for as-cast xSIBS, 102 nm for platelet-exposed xSIBS, 19 nm for PCL, and 0.3 nm for PMMA.

3.2. Shear-Induced Platelet Activation. Gel-filtered platelets were exposed to xSIBS, PCL, or PMMA at 1 dyn/cm² or 20 dyn/cm² for 12 min in the HSD, with platelet samples drawn every 4 min for the PAS assay. PAS increased with exposure time for all materials at both shear stress levels (Figure 6A). The change in PAS over the 12 min experimental duration, ΔPAS, was largest for xSIBS at 1 dyn/cm², while increasing the shear stress to 20 dyn/cm² yielded the largest ΔPAS for PCL, followed closely by xSIBS (Figure 6B). However, there was no difference between ΔPAS for the three materials for both shear stress levels ($n = 7$, $p > 0.05$).

We analyzed these results further in the context of shear-induced platelet sensitization, where platelets continue to

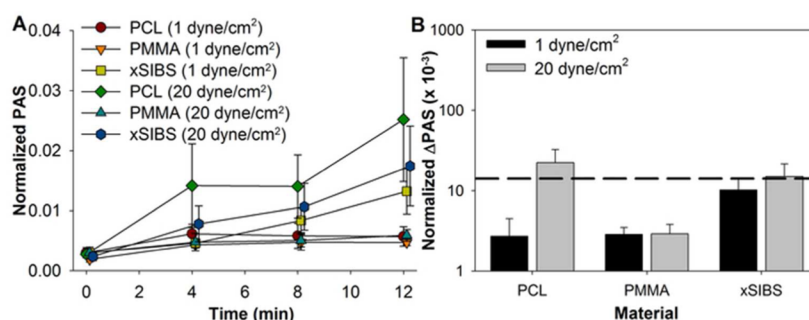


Figure 6. Shear-induced platelet activation in the HSD. GFP were exposed to 1 dyn/cm^2 or 20 dyn/cm^2 for 12 min in the HSD, with samples drawn every 4 min for the PAS assay. (A) PAS was observed to increase over the duration of the experiment, with the change in PAS (Δ PAS) over 12 min largest in the high flow rate regimes. (B) While the largest changes in PAS (Δ PAS) were measured for PCL and xSIBS at 20 dyn/cm^2 , no significant difference was observed ($p > 0.05$). The mean Δ PAS for xSIBS was slightly above the threshold observed for shear-induced platelet sensitization (dashed black line²⁶).

activate in low shear regions after initial high shear insult.²⁶ We selected a previously observed threshold PAS of 0.017, beyond which platelets were significantly activated.²⁶ Both xSIBS and PCL at 20 dyn/cm^2 yielded Δ PAS that was beyond this threshold, though this difference was minor.

3.3. Shear-Induced Platelet Adhesion. Platelet-rich plasma with a platelet count of 450 000/ μL was perfused over xSIBS, PCL, or PMMA in an acrylic parallel-plate flow chamber at a wall shear stress equivalent to 10 dyn/cm^2 for 5 min, after which the materials were fixed with glutaraldehyde and prepared for SEM imaging. Adhesion, calculated as adherent platelets per square millimeter, was observed for all materials ($n = 10$ images per experiment, 4 total experiments). PCL (Figure 7A) yielded significantly lower adhesion than both

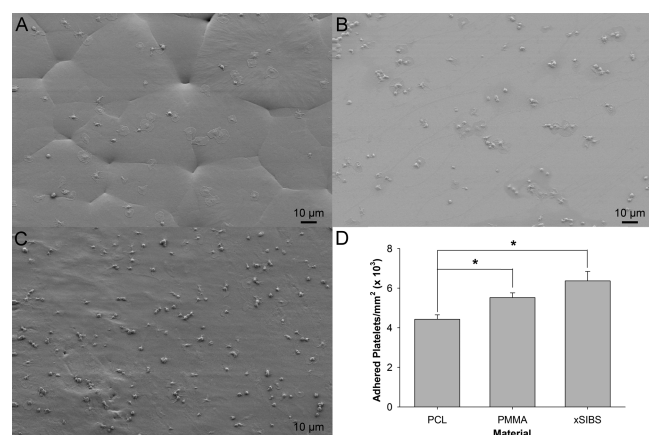


Figure 7. SEM images of adhered platelets after 5 min exposure of PRP to 10 dyn/cm^2 in a parallel plate flow chamber. The materials tested included (A) PCL, (B) PMMA, and (C) xSIBS. (D) xSIBS and PMMA yielded significantly higher platelet adhesion as compared to PCL ($*p < 0.05$).

PMMA (Figure 7B) and xSIBS (Figure 7C; $p < 0.05$). While xSIBS showed the most number of adherent platelets, no significant difference was observed in the adhesion level between PMMA and xSIBS (Figure 7D, $p > 0.05$). In general, most platelets were singly adhered to PCL and xSIBS, whereas clustering of platelets was largely observed on PMMA. Qualitatively, the phenotype of the adhered platelets ranged from ellipsoid to dendritic to fully spread for all materials. However, the resolution of the SEM images prohibited quantification of these different activation states as performed

in prior studies.³⁸ In addition, the SEM images clarify the topology of the materials as observed with AFM, with PCL displaying polygonal segmentation, PMMA showing a smooth amorphous surface, and xSIBS showing some sharp peaks separated by larger plateau regions.

4. DISCUSSION

The use of polymeric materials as fabrication substrates for prosthetic heart valves, as alternatives to xenografts, offers the promise of low thrombogenicity and high durability in a single device. Polymers may also be more suitable for development of a TAVR system, in terms of better withstanding crimping and deployment forces and offering hemodynamically optimized design configurations, which may in turn translate into expanded clinical indications for TAVR. The success of current polymers as suitable materials for PPHVs depends not only on their adaptation and durability in response to the dynamic flow conditions present in the native valvular region, but also their long-term biostability, hemocompatibility, and antithrombogenic response.³⁹ Major advances have been made in developing degradation-resistant polymers that have lower thrombogenic and calcification response, but these materials continue to lag in their hemodynamic response and long-term durability.^{39,40} In this study, we introduce a cross-linked version of SIBS (xSIBS) that potentially offers both the mechanical strength and low thrombogenic response required to be a viable PPHV material.

The UTS identifies the breaking strength of the polymer under uniaxial tensile conditions. The 35 MPa end point observed for xSIBS in this study is 24.5 times greater than the 1.43 MPa observed for the original SIBS Quatromer.⁶ The previously observed UTS for SIBS ranges from 10 to 30 MPa,¹ with a UTS of 20.7 MPa observed for SIBS with 24 mol % styrene content.⁴¹ The majority of polymer development for prosthetic heart valves focuses on polyurethanes (PU), with tensile strengths ranging from 20 to 90 MPa.⁴² However, due to biostability issues, chemically susceptible regions of PU have been modified, yielding poly(carbonate urethane) (PCU) and poly(ether urethane) (PEU), with UTS values of 48 and 82 MPa, respectively.⁴³ However, both undergo in vivo biodegradation, especially under flexion.⁴³ More recent modifications to PU include polyhedral oligomeric silsesquioxanes (POSS)-PCU, with mean UTS ranging from 31.0 to 55.9 MPa.¹⁸ Comparatively, the mean UTS of native aortic valve tissue is 2.6

Table 1. Surface Roughness and Contact Angles of Tested Biomaterials

material	as-cast xSIBS	platelet-exposed xSIBS	PCL	PMMA
roughness (nm)	144	102	19	0.3
contact angle (deg)	82.05 ± 0.02	88.27 ± 0.04	75.68 ± 0.30	70.13 ± 0.04

Surface roughness measurements were obtained using AFM. Contact angles were obtained using an optical contact angle meter and are represented as the mean and SD of 6 measurements. Shear and platelet exposure appeared to decrease the roughness and increase the contact angle of xSIBS.

MPa.⁴⁴ Thus, xSIBS has evolved into a stronger polymer via cross-linking, while still maintaining its biostability.

The AFM images of xSIBS (Figure 5A,B) appear to show amorphous glassy cylindrical segments, which represent polystyrene, interspersed with amorphous rubbery segments, representing isobutylene.¹ These features have been observed at the micro- and nanoscales in SIBS^{45–49} and other polyisobutylene-based polymers used in coronary stents.^{41,50,51} However, the heterogeneous microstructure may contribute to increased surface roughness causing enhanced platelet adhesion in some circumstances as discussed below.

Surface contact angle is used as a measure of surface wettability and may indicate the propensity of cells to adhere to the surface. Mean contact angles of 82.05 and 88.27° for as-cast and platelet-exposed xSIBS, respectively, are higher than the 72.34° observed for SIBS.⁸ The platelet-exposed xSIBS appears to be slightly more hydrophobic than the as-cast xSIBS, even though surface analysis by AFM yields lower roughness (Table 1). Contact angles for PEU, PCU, and POSS–PCU were observed to be 70, 69, and 82.6°, respectively.⁵² Both as-cast and platelet-exposed xSIBS have lower wettability than PCL and PMMA tested in this study, as well as the SIBS studied earlier; thus, their surfaces are considered hydrophobic. This may account for greater fibrinogen or von Willebrand factor adsorption, which may in turn account for increased platelet adhesion, as observed under flow conditions (Figure 7C). For example, the shear stress level used in the adhesion study is similar to the level, 0.8 Pa, at which greatest adhesion is observed for hydrophobic materials.^{53,54} The level of platelet adhesion may also be accounted for by the coupling of the material hydrophobicity with the relatively rougher surface of xSIBS, when compared with PCL and PMMA.⁵⁵ Prior platelet adhesion studies under flow conditions have shown that increased roughness on hydrophobic surfaces causes an increase in adhesion, whereas the opposite is true for hydrophilic materials.^{53,55} However, the increased thrombin generation, as defined by the Δ PAS, for xSIBS during exposure to 1 dyn/cm² is likely an effect of the chemical structure of xSIBS and not the surface roughness,⁵³ as both PCL and PMMA yield non-significantly lower Δ PAS at this shear stress level (Figure 6B). This effect is magnified as the shear stress is increased to 20 dyn/cm². Several studies have examined platelet adhesion on SIBS under flow at wall shear stresses equivalent to 3.5 and 35 dyn/cm².^{6,8} However, direct comparison with our results are not possible because these studies use an adhered platelet density based on the intensity of radioactively labeled platelets normalized against those adhered to PDMS⁶ or compared with SIBS whose surface had been modified with phospholipids.⁸ We compared the resulting Δ PAS to the level required for shear-induced platelet sensitization, whereupon platelets continue to activate at a greater rate as compared to platelets only exposed to low shear stress, even though the platelets are returned to “gentle” flow conditions.²⁶ Mean Δ PAS for platelets exposed to xSIBS at 1 dyn/cm² and 20 dyn/cm² is at or below this sensitization threshold for the 12 min exposure,

indicating an acceptable level of thrombin generation (Figure 6B). However, platelets exposed to PCL at 20 dyn/cm² exceed this threshold, indicating sensitized platelets that are susceptible to further activation, even at low shear stresses. It is important to note that the overall Δ PAS observed for all materials and shear conditions is approximately 1% or less of the maximum thrombin-generating potential of the shear-exposed platelets, and no significance in Δ PAS values were observed for either the materials or shear stress levels, indicating low thrombogenicity. Furthermore, normal thrombin (4 ng/mL) has a half-life of 56.4 s, which can be extended to 168.2 s for antithrombin deficient plasma.⁵⁶ However, the PAS assay utilizes acetylated prothrombin, which generates defective thrombin that is incapable of further activating platelets or participation in the generation of insoluble fibrin and may have an extended half-life. In addition, the assay provides 10 μ M acetylated prothrombin to ensure sufficient substrate for thrombin generation.³⁵

PCL has been examined as a potential scaffold material for tissue-engineered aortic valves³⁰ and for cell delivery during cardiovascular tissue engineering applications due to its cell seeding efficiency and slow in vivo biodegradability.^{57,58} PCL has low roughness and is hydrophobic,⁵⁹ with higher protein adsorption and platelet adhesion under static incubation when compared to glass,⁵⁹ composites with other biomaterials,^{59,60} and materials with surface modifications.^{61,62} Exposure to PCL on an orbital shaker at 100 rpm for 2 h yielded approximately 6000 adhered platelets/cm², with the majority of platelets exhibiting partial activation, short dendrites, and no clustering.³¹ The fluid shear-exposed platelets in our study exhibited both partially activated and spread platelets, but with a 66-fold increase in the number of adherent platelets. Furthermore, PCL yielded low platelet activity under 1 dyn/cm² shear stress exposure, but the Δ PAS over the 12 min experimental duration increased 8-fold after exposure to 20 dyn/cm², potentially a result of disturbed flow due to the fragmented PCL surface.

PMMA (brand named as Plexiglas) has been used for a variety of biomedical applications due to its chemical stability and inertness.³⁴ Such applications included the housing and cage for the Hufnagel and original Starr–Edwards valves, respectively.⁶³ However, PMMA is also hydrophobic and has a high water contact angle. Consequently, PMMA has yielded higher P-selectin,³² thrombin generation,³³ and platelet adhesion^{32–34} under static conditions when compared to materials such as PU, low density polyethylene (LDPE), and nanostructured PMMA. Adhered platelets on PMMA films yielded an irregular spread phenotype with clustering.³² In this study, PMMA-exposed platelets exhibited a similar spread and clustering behavior as previously observed, and with significantly greater platelet adhesion than PCL. However, under 1 and 20 dyn/cm² shear stress, PMMA yielded lower Δ PAS than both PCL and xSIBS, indicating that PMMA is not highly platelet-activating under flow conditions. This may be partially explained by the lowest roughness observed for PMMA when compared to the other materials tested.

The use of isolated platelets in our studies (i.e., free of plasma protein constituents) ensured that the measured platelet activation was only a function of the fluid shear stress, exposure time, and material contact. However, further experiments may be conducted using reconstituted whole blood (without plasma proteins) and measuring the PAS,⁶⁴ or whole blood and measuring P-selectin expression.⁶⁵ We exposed isolated platelets to 1 and 20 dyn/cm² in activation experiments and PRP to 10 dyn/cm² in adhesion experiments to emulate the shear stress conditions found in a variety of blood vessels and vascular prostheses.⁶⁶ While platelets encounter fluid shear stresses on the order of 1×10^3 dyn/cm² in prosthetic heart valves,⁴⁰ we chose to use low constant shear stress conditions in order to examine the synergistic response to both shear stress and material contact that may be obscured by device-related flow conditions.⁶⁶ Shear-induced platelet activation, particularly at levels above 60–80 dyn/cm², has been observed to stimulate increased platelet deposition, stable aggregation, and thrombosis onto biomaterials.⁶⁶ Prior studies have mitigated the hydrophobicity of SIBS and reduced platelet adhesion by sulfonation^{9,67} and coating with 1,2-dimyristoyl-rac-glycero-3-phosphocholine (DMPC).⁸ Furthermore, the roughness of the xSIBS sheets may also play a role in platelet adhesion. The surface roughness reported here may be mitigated by refining the manufacturing process.⁶⁸ Platelet adhesion on other valve polymer candidates (such as thermoplastic polyurethane, PCU, and silicone) has been reduced by surface smoothing of thermoplastic polyurethane with argon plasma treatment,⁶⁹ transfer of a wave-like groove pattern to PCU tubes from a centrifugal casting mold,⁷⁰ and magnetic abrasive finishing of silicone rubber.⁷¹ Optimization of xSIBS roughness using similar techniques will be explored in the future. The role of microstructured surfaces in mitigation of platelet adhesion has been demonstrated on poly(lactic-co-glycolic-acid) (PLGA) films,⁷² and the generation of microstructures has been implemented via slow injection molding for poly(styrene-block-isoprene-block-styrene) (SIS30), which is structurally similar to SIBS.⁷³ In addition to these modifications, the biocompatibility of xSIBS will be further analyzed for endotoxin load using a limulus amoebocyte lysate (LAL) test, as well as cytotoxicity, as per ISO 10993-5 standards. Future studies examining platelet adhesion under flow conditions will statistically analyze the activation state phenotype, as performed by prior studies.³⁸

While our primary objective is to develop a durable and hemocompatible polymer for heart valve prostheses, the mechanical and hemocompatibility characteristics of xSIBS may make it suitable for cardiovascular applications with similar requirements.¹ Furthermore, the mechanical and thrombogenicity tests and relevant tools, such as the Hemodynamic Shearing Device and parallel platelet flow chamber, may be used in future approaches to optimize the mechanical function and properties of xSIBS and other valve polymer candidates while minimizing their thrombogenic response. These approaches for measuring flow-induced platelet response may be a better representation of “in-use” behavior of biomaterials compared to the commonly used static platelet exposure tests.⁷⁴

5. CONCLUSIONS

We prepared and examined the mechanical, surface, and hemocompatibility properties of xSIBS, a thermally cross-linked version of SIBS, which has previously been shown to be “super

biostable”. This novel thermoset formulation, which involved the addition of 4-VBCB to induce cross-linking, generated xSIBS with ultimate tensile strength that was superior to prior versions of SIBS and comparable to other classes of polymers, such as PU, developed for PPHVs. While the xSIBS utilized in this study exhibited a hydrophobic nature, as indicated by large contact angles and significant roughness, its flow-mediated platelet activation and adhesion response was similar to PCL and PMMA, which have a history of successful use for blood-contacting applications. The strong mechanical and low thrombogenic properties of xSIBS, coupled with its superior biostability, therefore, make it a viable candidate for use in PPHVs.

■ AUTHOR INFORMATION

Corresponding Author

*Tel.: (631) 444-2156. Fax: (631) 444-7530. E-mail: danny.bluestein@stonybrook.edu.

Author Contributions

The manuscript was written through contributions of all authors. All authors have given approval to the final version of the manuscript.

Funding

This work was supported by the NIH-NIBIB Quantum Program (Award No. 5U01EB012487–04, DB).

Notes

The authors declare the following competing financial interest(s): Drs. Bluestein, Claiborne, and Slepian are co-founders and shareholders of Polynova Cardiovascular, Inc. Drs. Pinchuk and Kato are shareholders of Innovia LLC, the manufacturer of xSIBS.

■ ACKNOWLEDGMENTS

The authors wish to thank Dr. Syed F. Hossainy, Ph.D., of Abbott Vascular for his consultation regarding platelet-biomaterial interactions under shear flows.

■ REFERENCES

- (1) Pinchuk, L.; Wilson, G. J.; Barry, J. J.; Schoepfoerster, R. T.; Parel, J. M.; Kennedy, J. P. Medical Applications of Poly(Styrene-Block-Isobutylene-Block-Styrene) (“Sibs”). *Biomaterials* **2008**, *29*, 448–460.
- (2) El Fray, M.; Prowans, P.; Puskas, J. E.; Altstadt, V. Biocompatibility and Fatigue Properties of Polystyrene-Polyisobutylene-Polystyrene, an Emerging Thermoplastic Elastomeric Biomaterial. *Biomacromolecules* **2006**, *7*, 844–850.
- (3) Claiborne, T. E.; Girdhar, G.; Gallocher-Lowe, S.; Sheriff, J.; Kato, Y. P.; Pinchuk, L.; Schoepfoerster, R. T.; Jesty, J.; Bluestein, D. Thrombogenic Potential of Innovia Polymer Valves Versus Carpentier-Edwards Perimount Magna Aortic Bioprosthetic Valves. *ASAIO J.* **2011**, *57*, 26–31.
- (4) Claiborne, T. E.; Bluestein, D.; Schoepfoerster, R. T. Development and Evaluation of a Novel Artificial Catheter-Deliverable Prosthetic Heart Valve and Method for in Vitro Testing. *Int. J. Artif. Organs* **2009**, *32*, 262–271.
- (5) Wang, Q.; McGoron, A. J.; Bianco, R.; Kato, Y.; Pinchuk, L.; Schoepfoerster, R. T. In-Vivo Assessment of a Novel Polymer (SIBS) Trileaflet Heart Valve. *J. Heart Valve Dis.* **2010**, *19*, 499–505.
- (6) Gallocher, S. L.; Aguirre, A. F.; Kasyanov, V.; Pinchuk, L.; Schoepfoerster, R. T. A Novel Polymer for Potential Use in a Trileaflet Heart Valve. *J. Biomed. Mater. Res., Part B* **2006**, *79*, 325–334.
- (7) Wang, Q.; McGoron, A. J.; Pinchuk, L.; Schoepfoerster, R. T. A Novel Small Animal Model for Biocompatibility Assessment of

Polymeric Materials for Use in Prosthetic Heart Valves. *J. Biomed. Mater. Res., Part A* **2010**, *93*, 442–453.

(8) Duraiswamy, N.; Choksi, T. D.; Pinchuk, L.; Schoepfoerster, R. T. A Phospholipid-Modified Polystyrene-Polyisobutylene-Polystyrene (Sibs) Triblock Polymer for Enhanced Hemocompatibility and Potential Use in Artificial Heart Valves. *J. Biomater. Appl.* **2009**, *23*, 367–379.

(9) Zhu, J. Z.; Xiong, X. W.; Du, R.; Jing, Y. J.; Ying, Y.; Fan, X. M.; Zhu, T. Q.; Zhang, R. Y. Hemocompatibility of Drug-Eluting Coronary Stents Coated with Sulfonated Poly (Styrene-Block-Isobutylene-Block-Styrene). *Biomaterials* **2012**, *33*, 8204–8212.

(10) Zhou, Y.; Pinchuk, L. *Crosslinked Polyolefins for Biomedical Applications and Method of Making Same*. U.S. Patent 8,765,895 B2, 2014.

(11) Vesely, I. The Influence of Design on Bioprosthetic Valve Durability. *J. Long-Term Eff. Med. Implants* **2001**, *11*, 137–149.

(12) Vesely, I. The Evolution of Bioprosthetic Heart Valve Design and Its Impact on Durability. *Cardiovasc. Pathol.* **2003**, *12*, 277–286.

(13) Claiborne, T. E.; Xenos, M.; Sheriff, J.; Chiu, W. C.; Soares, J.; Alemu, Y.; Gupta, S.; Judex, S.; Slepian, M. J.; Bluestein, D. Toward Optimization of a Novel Trileaflet Polymeric Prosthetic Heart Valve Via Device Thrombogenicity Emulation. *ASAIO J.* **2013**, *59*, 275–283.

(14) Claiborne, T. E.; Sheriff, J.; Kuetting, M.; Steinseifer, U.; Slepian, M. J.; Bluestein, D. In Vitro Evaluation of a Novel Hemodynamically Optimized Trileaflet Polymeric Prosthetic Heart Valve. *J. Biomech. Eng.* **2013**, *135*, 021021.

(15) Kütting, M.; Roggenkamp, J.; Urban, U.; Schmitz-Rode, T.; Steinseifer, U. Polyurethane Heart Valves: Past, Present and Future. *Expert Rev. Med. Devices* **2011**, *8*, 227–233.

(16) Bezuidenhout, D.; Williams, D. F.; Zilla, P. Polymeric Heart Valves for Surgical Implantation, Catheter-Based Technologies and Heart Assist Devices. *Biomaterials* **2015**, *36*, 6–25.

(17) Claiborne, T. E.; Slepian, M. J.; Hossainy, S.; Bluestein, D. Polymeric Trileaflet Prosthetic Heart Valves: Evolution and Path to Clinical Reality. *Expert Rev. Med. Devices* **2012**, *9*, 577–594.

(18) Rahmani, B.; Tzamtzis, S.; Ghanbari, H.; Burriesci, G.; Seifalian, A. M. Manufacturing and Hydrodynamic Assessment of a Novel Aortic Valve Made of a New Nanocomposite Polymer. *J. Biomech* **2012**, *45*, 1205–1211.

(19) Webb, J. G.; Wood, D. A. Current Status of Transcatheter Aortic Valve Replacement. *J. Am. Coll. Cardiol.* **2012**, *60*, 483–492.

(20) Alavi, S. H.; Groves, E. M.; Kheradvar, A. The Effects of Transcatheter Valve Crimping on Pericardial Leaflets. *Ann. Thorac Surg* **2014**, *97*, 1260–1266.

(21) Kiefer, P.; Gruenwald, F.; Kempfert, J.; Aupperle, H.; Seeburger, J.; Mohr, F. W.; Walther, T. Crimping May Affect the Durability of Transcatheter Valves: An Experimental Analysis. *Ann. Thorac Surg* **2011**, *92*, 155–160.

(22) Amahzoune, B.; Bruneval, P.; Allam, B.; Lafont, A.; Fabiani, J. N.; Zegdi, R. Traumatic Leaflet Injury During the Use of Percutaneous Valves: A Comparative Study of Balloon- and Self-Expandable Valved Stents. *Eur. J. Cardiothorac. Surg.* **2013**, *43*, 488–493.

(23) Zegdi, R.; Bruneval, P.; Blanchard, D.; Fabiani, J. N. Evidence of Leaflet Injury During Percutaneous Aortic Valve Deployment. *Eur. J. Cardiothorac. Surg.* **2011**, *40*, 257–259.

(24) de Buhr, W.; Pfeifer, S.; Slotta-Huspenina, J.; Wintermantel, E.; Lutter, G.; Goetz, W. A. Impairment of Pericardial Leaflet Structure from Balloon-Expanded Valved Stents. *J. Thorac. Cardiovasc. Surg.* **2012**, *143*, 1417–1421.

(25) Nobili, M.; Sheriff, J.; Morbiducci, U.; Redaelli, A.; Bluestein, D. Platelet Activation Due to Hemodynamic Shear Stresses: Damage Accumulation Model and Comparison to in Vitro Measurements. *ASAIO J.* **2008**, *54*, 64–72.

(26) Sheriff, J.; Bluestein, D.; Girdhar, G.; Jesty, J. High-Shear Stress Sensitizes Platelets to Subsequent Low-Shear Conditions. *Ann. Biomed. Eng.* **2010**, *38*, 1442–1450.

(27) Sheriff, J.; Girdhar, G.; Chiu, W. C.; Jesty, J.; Slepian, M. J.; Bluestein, D. Comparative Efficacy of in Vitro and in Vivo Metabolized

Aspirin in the DeBakey Ventricular Assist Device. *J. Thromb. Thrombolysis* **2014**, *37*, 499–506.

(28) Sheriff, J.; Soares, J. S.; Xenos, M.; Jesty, J.; Bluestein, D. Evaluation of Shear-Induced Platelet Activation Models under Constant and Dynamic Shear Stress Loading Conditions Relevant to Devices. *Ann. Biomed. Eng.* **2013**, *41*, 1279–1296.

(29) Soares, J. S.; Sheriff, J.; Bluestein, D. A Novel Mathematical Model of Activation and Sensitization of Platelets Subjected to Dynamic Stress Histories. *Biomech. Model. Mechanobiol.* **2013**, *12*, 1127–1141.

(30) Van Lieshout, M.; Peters, G.; Rutten, M.; Baaijens, F. A Knitted, Fibrin-Covered Polycaprolactone Scaffold for Tissue Engineering of the Aortic Valve. *Tissue Eng.* **2006**, *12*, 481–487.

(31) Leszczak, V.; Smith, B. S.; Popat, K. C. Hemocompatibility of Polymeric Nanostructured Surfaces. *J. Biomater. Sci., Polym. Ed.* **2013**, *24*, 1529–1548.

(32) Shih, M. F.; Shau, M. D.; Chang, M. Y.; Chiou, S. K.; Chang, J. K.; Cherng, J. Y. Platelet Adsorption and Hemolytic Properties of Liquid Crystal/Composite Polymers. *Int. J. Pharm. (Amsterdam, Neth.)* **2006**, *327*, 117–125.

(33) Nurdin, N.; Francois, P.; Mugnier, Y.; Krumeich, J.; Moret, M.; Aronsson, B. O.; Descouts, P. Haemocompatibility Evaluation of DLC- and SIC-Coated Surfaces. *Eur. Cells Mater.* **2003**, *5*, 17–26.

(34) Serizawa, T.; Yamashita, K.; Akashi, M. Cell-Adhesive and Blood-Coagulant Properties of Ultrathin Poly(Methyl Methacrylate) Stereocomplex Films. *J. Biomater. Sci., Polym. Ed.* **2004**, *15*, 511–526.

(35) Jesty, J.; Bluestein, D. Acetylated Prothrombin as a Substrate in the Measurement of the Procoagulant Activity of Platelets: Elimination of the Feedback Activation of Platelets by Thrombin. *Anal. Biochem.* **1999**, *272*, 64–70.

(36) Xenos, M.; Girdhar, G.; Alemu, Y.; Jesty, J.; Slepian, M.; Einav, S.; Bluestein, D. Device Thrombogenicity Emulator (Dte) - Design Optimization Methodology for Cardiovascular Devices: A Study in Two Bileaflet Mhv Designs. *J. Biomech* **2010**, *43*, 2400–2409.

(37) Schulz-Heik, K.; Ramachandran, J.; Bluestein, D.; Jesty, J. The Extent of Platelet Activation under Shear Depends on Platelet Count: Differential Expression of Anionic Phospholipid and Factor Va. *Pathophysiol. Haemostasis Thromb.* **2005**, *34*, 255–262.

(38) Braune, S.; Honow, A.; Mrowietz, C.; Cui, J.; Kratz, K.; Hellwig, J.; Uzum, C.; Klitzing, R. V.; Lendlein, A.; Jung, F. Hemocompatibility of Soft Hydrophobic Poly(N-Butyl Acrylate) Networks with Elastic Moduli Adapted to the Elasticity of Human Arteries. *Clin. Hemorheol. Microcirc.* **2011**, *49*, 375–390.

(39) Ghanbari, H.; Viatge, H.; Kidane, A. G.; Burriesci, G.; Tavakoli, M.; Seifalian, A. M. Polymeric Heart Valves: New Materials, Emerging Hopes. *Trends Biotechnol.* **2009**, *27*, 359–367.

(40) Kuan, Y. H.; Dasi, L. P.; Yoganathan, A.; Leo, H. L. Recent Advances in Polymeric Heart Valves Research. *Int. J. Biomat. Res. Eng.* **2011**, *1*, 1–17.

(41) Strickler, F.; Richard, R.; McFadden, S.; Lindquist, J.; Schwarz, M. C.; Faust, R.; Wilson, G. J.; Boden, M. In Vivo and in Vitro Characterization of Poly(Styrene-B-Isobutylene-B-Styrene) Copolymer Stent Coatings for Biostability, Vascular Compatibility and Mechanical Integrity. *J. Biomed. Mater. Res., Part A* **2010**, *92*, 773–782.

(42) Kidane, A. G.; Burriesci, G.; Cornejo, P.; Dooley, A.; Sarkar, S.; Bonhoeffer, P.; Edirisinghe, M.; Seifalian, A. M. Current Developments and Future Prospects for Heart Valve Replacement Therapy. *J. Biomed. Mater. Res., Part B* **2009**, *88*, 290–303.

(43) Christenson, E. M.; Dadsetan, M.; Wiggins, M.; Anderson, J. M.; Hiltner, A. Poly(Carbonate Urethane) and Poly(Ether Urethane) Biodegradation: In Vivo Studies. *J. Biomed. Mater. Res.* **2004**, *69*, 407–416.

(44) Balguid, A.; Rubbens, M. P.; Mol, A.; Bank, R. A.; Bogers, A. J.; van Kats, J. P.; de Mol, B. A.; Baaijens, F. P.; Bouten, C. V. The Role of Collagen Cross-Links in Biomechanical Behavior of Human Aortic Heart Valve Leaflets—Relevance for Tissue Engineering. *Tissue Eng.* **2007**, *13*, 1501–1511.

- (45) Storey, R. F.; Chisholm, B. J.; Masse, M. A. Morphology and Physical Properties of Poly(Styrene-*B*-Isobutylene-*B*-Styrene) Block Copolymers. *Polymer* **1996**, *37*, 2925–2938.
- (46) Ranade, S. V.; Richard, R. E.; Helmus, M. N. Styrenic Block Copolymers for Biomaterial and Drug Delivery Applications. *Acta Biomater.* **2005**, *1*, 137–144.
- (47) Ren, P.; Wu, Y. B.; Guo, W. L.; Li, S. X.; Mao, J.; Xiao, F.; Li, K. Synthesis, Characterization and Haemocompatibility of Poly(styrene-*b*-isobutylene-*b*-styrene) Triblock Copolymers. *Polymer (Korea)* **2011**, *35*, 40–46.
- (48) Puskas, J. E.; Antony, P.; Kwon, Y.; Kovar, M.; Norton, P. R. Study of the Surface Morphology of Polyisobutylene-Based Block Copolymers by Atomic Force Microscopy. *Macromol. Symp.* **2002**, *183*, 191–197.
- (49) Antony, P.; Puskas, J. E.; Kontopoulou, M. Investigation of the Rheological and Mechanical Properties of a Polystyrene-Polyisobutylene-Polystyrene Triblock Copolymer and Its Blends with Polystyrene. *Polym. Eng. Sci.* **2003**, *43*, 243–253.
- (50) Ojha, U.; Kulkarni, P.; Faust, R. Syntheses and Characterization of Novel Biostable Polyisobutylene Based Thermoplastic Polyurethanes. *Polymer* **2009**, *50*, 3448–3457.
- (51) Richard, R. E.; Faust, R. *Medical Devices and Materials Containing Isobutylene Copolymer*. U.S. Patent 8,697,119 B2, 2014.
- (52) Kannan, R. Y.; Salacinski, H. J.; Ghanavi, J. E.; Narula, A.; Odlyha, M.; Peirovi, H.; Butler, P. E.; Seifalian, A. M. Silsesquioxane Nanocomposites as Tissue Implants. *Plast. Reconstr. Surg.* **2007**, *119*, 1653–1662.
- (53) van Oeveren, W. Obstacles in Haemocompatibility Testing. *Scientifica* **2013**, *2013*, 392584.
- (54) Spijker, H. T.; Bos, R.; Busscher, H. J.; Graaff, R.; van Oeveren, W. Adhesion of Blood Platelets under Flow to Wettability Gradient Polyethylene Surfaces Made in a Shielded Gas Plasma. *J. Adhes. Sci. Technol.* **2002**, *16*, 1703–1713.
- (55) Zingg, W.; Neumann, A. W.; Strong, A. B.; Hum, O. S.; Absolom, D. R. Effect of Surface Roughness on Platelet Adhesion under Static and under Flow Conditions. *Can. J. Surg.* **1982**, *25*, 16–19.
- (56) Ruhl, H.; Muller, J.; Harbrecht, U.; Fimmers, R.; Oldenburg, J.; Mayer, G.; Potzsch, B. Thrombin Inhibition Profiles in Healthy Individuals and Thrombophilic Patients. *Thromb. Haemostasis* **2012**, *107*, 848–853.
- (57) Woodruff, M. A.; Huttmacher, D. W. The Return of a Forgotten Polymer-Polycaprolactone in the 21st Century. *Prog. Polym. Sci.* **2010**, *35*, 1217–1256.
- (58) Slepian, M. J. Polymeric Endoluminal Paving. A Family of Evolving Methods for Extending Endoluminal Therapeutics Beyond Stenting. *Cardiol. Clin.* **1994**, *12*, 715–737.
- (59) Hsu, S. H.; Tang, C. M.; Lin, C. C. Biocompatibility of Poly(Epsilon-Caprolactone)/Poly(Ethylene Glycol) Diblock Copolymers with Nanophase Separation. *Biomaterials* **2004**, *25*, 5593–5601.
- (60) Liu, L.; Guo, S. R.; Chang, J.; Ning, C. Q.; Dong, C. M.; Yan, D. Y. Surface Modification of Polycaprolactone Membrane Via Layer-by-Layer Deposition for Promoting Blood Compatibility. *J. Biomed. Mater. Res., Part B* **2008**, *87B*, 244–250.
- (61) Khandwekar, A. P.; Patil, D. P.; Shouche, Y.; Doble, M. Surface Engineering of Polycaprolactone by Biomacromolecules and Their Blood Compatibility. *J. Biomater. Appl.* **2011**, *26*, 227–252.
- (62) Jiang, H.; Wang, X. B.; Li, C. Y.; Li, J. S.; Xu, F. J.; Mao, C.; Yang, W. T.; Shen, J. Improvement of Hemocompatibility of Polycaprolactone Film Surfaces with Zwitterionic Polymer Brushes. *Langmuir* **2011**, *27*, 11575–11581.
- (63) Mohammadi, H.; Mequanint, K. Prosthetic Aortic Heart Valves: Modeling and Design. *Med. Eng. Phys.* **2011**, *33*, 131–147.
- (64) Girdhar, G.; Xenos, M.; Alemu, Y.; Chiu, W. C.; Lynch, B. E.; Jesty, J.; Einav, S.; Slepian, M. J.; Bluestein, D. Device Thrombogenicity Emulation: A Novel Method for Optimizing Mechanical Circulatory Support Device Thromboresistance. *PLoS One* **2012**, *7*, e32463.
- (65) Gemmell, C. H. Activation of Platelets by in Vitro Whole Blood Contact with Materials: Increases in Microparticle, Procoagulant Activity, and Soluble P-Selectin Blood Levels. *J. Biomater. Sci., Polym. Ed.* **2001**, *12*, 933–943.
- (66) Spijker, H. T.; Graaff, R.; Boonstra, P. W.; Busscher, H. J.; van Oeveren, W. On the Influence of Flow Conditions and Wettability on Blood Material Interactions. *Biomaterials* **2003**, *24*, 4717–4727.
- (67) Suleiman, D.; Padovani, A. M.; Negrón, A. A.; Sloan, J. M.; Napadensky, E.; Crawford, D. M. Mechanical and Chemical Properties of Poly(Styrene-Isobutylene-Styrene) Block Copolymers: Effect of Sulfonation and Counter Ion Substitution. *J. Appl. Polym. Sci.* **2014**, *131*, 40344.
- (68) Braune, S.; Lange, M.; Richau, K.; Lutzow, K.; Weigel, T.; Jung, F.; Lendlein, A. Interaction of Thrombocytes with Poly(ether imide): The Influence of Processing. *Clin. Hemorheol. Microcirc.* **2010**, *46*, 239–250.
- (69) Alves, P.; Cardoso, R.; Correia, T. R.; Antunes, B. P.; Correia, I. J.; Ferreira, P. Surface Modification of Polyurethane Films by Plasma and Ultraviolet Light to Improve Haemocompatibility for Artificial Heart Valves. *Colloids Surf., B* **2014**, *113*, 25–32.
- (70) Clauser, J.; Gester, K.; Roggenkamp, J.; Mager, I.; Maas, J.; Jansen, S. V.; Steinseifer, U. Micro-Structuring of Polycarbonate-Urethane Surfaces in Order to Reduce Platelet Activation and Adhesion. *J. Biomater. Sci., Polym. Ed.* **2014**, *25*, 504–518.
- (71) Boggs, T.; Carroll, R.; Tran-Son-Tay, R.; Yamaguchi, H.; Al-Mousily, F.; DeGroff, C. Blood Cell Adhesion on a Polymeric Heart Valve Leaflet Processed Using Magnetic Abrasive Finishing. *J. Med. Devices* **2014**, 8.01100510.1115/1.4025853
- (72) Koh, L. B.; Rodriguez, I.; Venkatraman, S. S. The Effect of Topography of Polymer Surfaces on Platelet Adhesion. *Biomaterials* **2010**, *31*, 1533–1545.
- (73) Stasiak, J.; Brubert, J.; Serrani, M.; Nair, S.; de Gaetano, F.; Costantino, M. L.; Moggridge, G. D. A Bio-Inspired Microstructure Induced by Slow Injection Moulding of Cylindrical Block Copolymers. *Soft Matter* **2014**, *10*, 6077–6086.
- (74) Furukawa, K. S.; Nakamura, K.; Onimura, Y.; Uchida, M.; Ito, A.; Yamane, T.; Tamaki, T.; Ushida, T.; Tateishi, T. Quantitative Analysis of Human Platelet Adhesions under a Small-Scale Flow Device. *Artif. Organs* **2010**, *34*, 295–300.